NIH Public Access
Author Manuscript
J Recept Signal Transduct Res. Author manuscript; available in PMC 2010 August 16.

Published in final edited form as:
J Recept Signal Transduct Res. 2010 April ; 30(2): 78–87. doi:10.3109/10799891003614808.

Cardiac specific deletion of *N*-methyl-$_D$-aspartate receptor 1 ameliorates mtMMP-9 mediated autophagy/mitophagy in hyperhomocysteinemia

Neetu Tyagi, **Jonathan C. Vacek**, **Srikanth Givvimani**, **Utpal Sen**, and **Suresh C. Tyagi**
Department of Physiology and Biophysics, School of Medicine, University of Louisville, Louisville, KY, USA

Abstract

Autophagy is an important process in the pathogenesis of cardiovascular diseases; however, the proximal triggers for mitochondrial autophagy were unknown. The *N*-methyl-$_D$-aspartate receptor 1 (NMDA-R1) is a receptor for homocysteine (Hcy) and plays a key role in cardiac dysfunction. Cardiac-specific deletion of NMDA-R1 has been shown to ameliorate Hcy-induced myocyte contractility. Hcy activates mitochondrial matrix metalloproteinase-9 (mtMMP-9) and induces translocation of connexin-43 (Cxn-43) to the mitochondria (mtCxn-43). We sought to show cardiac-specific deletion of NMDA-R1 mitigates Hcy-induced mtCxn-43 translocation, mtMMP-9-mediated mtCxn-43 degradation, leading to mitophagy, in part, by decreasing mitochondrial permeability (MPT). Cardiac-specific knockout (KO) of NAMDA-R1 was generated using the cre/lox approach. The myocyte mitochondria were isolated from wild type (WT), WT + Hcy (1.8 g of DL-Hcy/L in the drinking water for 6 weeks), NMDA-R1 KO + Hcy, and $NR1^{fl/fl}$/Cre ($NR1^{fl/fl}$) genetic control mice. Mitochondrial respiratory capacity and MPT were measured by fluorescence-dye methods. The mitochondrial superoxide and peroxinitrite levels were detected by confocal microscopy using Mito-SOX and dihydrorhodamine-123. The mtMMP-9 activity and expression were detected by zymography and RT-PCR analyses. The mtCxn-43 translocation was detected by confocal microscopy. The degradation of mtCxn-43 and LC3-I/II (a marker of autophagy) were detected by Western blot. These results suggested that Hcy enhanced intramitochondrial nitrosative stress in myocytes. There was a robust increase in mtMMP-9 activity. An increase in translocation and degradation of mtCxn-43 was also noted. These increases led to mitophagy. The effects were ameliorated by cardiac-specific deletion of NMDA-R1. We concluded that HHcy increased mitochondrial nitrosative stress, thereby activating mtMMP-9 and inciting the degradation of mtCxn-43. This led to mitophagy, in part, by activating NMDA-R1. The findings of this study will lead to therapeutic ramifications for mitigating cardiovascular diseases by inhibiting the mitochondrial mitophagy and NMDA-R1 receptor.

Keywords

Mitochondrial MMP; mitochondrial connexin-43 and microtubule-associated protein light chain 3; nitrosative stress

© 2010 Informa UK Ltd

Address for Correspondence: Suresh C. Tyagi, Department of Physiology and Biophysics, Health Sciences Center, A-1115, University of Louisville, Louisville, KY 40292, USA. suresh.tyagi@louisville.edu.

Declaration of interest
The authors report no conflicts of interest. The corresponding author are responsible for the content and writing of the paper.

NIH-PA Author Manuscript
NIH-PA Author Manuscript
NIH-PA Author Manuscript

NIH-PA Author Manuscript

NIH-PA Author Manuscript

NIH-PA Author Manuscript

Introduction

Homocysteine (Hcy) is a sulfur-containing non-protein amino acid formed during the intracellular conversion of methionine to cysteine. Deficiency in folic acid, vitamin B6, and vitamin B12 lead to hyperhomocysteinemia (HHcy) (1). HHcy is directly associated with the induction of arrhythmias. Cardiac arrhythmias lead to sudden cardiac death (SCD) and the blockade of *N*-methyl-D-aspartate receptor 1 (NMDA-R1) receptors mitigated SCD (2,3).

NMDA-R1 is present in the mammalian neurons (4), cardiomyocytes (5), and the endothelial cell (6). The activation of NMDA-R induced mitochondrial oxidative stress and calcium influx lead to cell death (7). The antagonist to NMDA receptor protected against an increase in heart rate induced by NMDA analog (8). This result suggested that Hcy was a NMDA receptor agonist.

Mitochondrial translocation of calpain (calcium-dependent cysteine proteases) induced NADPH oxidase-4 (NOX-4) and down-regulated thioredoxin-2 (TRX-2) in HHcy (9) leading to intramitochondrial oxidative stress. The tPA (serine protease) caused ECM degradation and proteolytic shedding of NMDA-R (10). The NMDA-R antagonist inhibited MMP activation and attenuated heart failure (11). MMPs are membrane-bound zinc-dependent endoproteinases (12). MMPs active site is bound with nitric oxide. Most of the MMPs in the heart are in the latent form and are activated by Hcy. Activation of MMPs caused a decrease in eNO bio-availability, which increased ROS and generated peroxynitrite (13). MMP activation in HHcy decreased elastin/collagen ratio, increased the deposition of interstitial collagen (fibrosis) between endothelium and myocytes and was arrhythmogenic (14,15). We and others have shown the presence of MMP in cardiac mitochondria (16,17). However, the physiological consequences of mtMMP activation were not well understood.

HHcy also changed the intercellular communication through gap junction channels formation by connexins (18). It is known that an elevated level of Hcy-induced extracellular matrix remodeling, which is responsible for altering the gap junction proteins (connexins), thereby increasing arrhythmias (19). Connexin-43 (Cxn-43) is a primary gap junction channel protein that plays a major role in electrical coupling in the ventricle. Cxn-43 is redistributed in heart with diseases such as infarction and hypertrophy (20,21). In contradiction, Hcy increased nitrosylation of Cxn-43 and increased its expression, which was then degraded in the mitochondria (22). Cxn-43 is found to be present in the inner membrane of myocyte mitochondria (mtCxn-43) and found to be cardioprotective during ischemia/reperfusion injury (23). Studies suggested that the moderate reduction in mitochondrial Cxn-43 abolished the protection induced by diazoxide (24). MMP activation degraded Cxn-43 leading to electrical conduction malfunction (25). Cxn channels are voltage-gated and can sense mitochondrial permeability transition pore. However, the physiological consequences of the Cxn-43 translocation and degradation in the mitochondria are not understood.

The mitochondrial permeability transition pore played an important role in mitophagy. Mitophagy is an intracellular process that is involved in the removal of mitochondria by autophagy (26). Mitophagy occurred constitutively in the normal myocardium, and disruption of this pathway resulted in the development of left ventricular infarction and severe myocyte dysfunction in the presence of any stress (27). Recently LPS was reported to stimulate mitochondrial autophagy in neonatal rat cardiomyocytes (28). There were evidences that mitophagy increased in various pathological conditions including cardiomyopathy and heart failure (29). However, the mechanism of mitophagy was unclear. We speculated that Hcy increased the mitochondrial oxidative nitrosative stresses, activated mtMMP, and degraded mtCxn-43 leading to mitochondrial mitophagy, in part, by opening

NIH-PA Author Manuscript

NIH-PA Author Manuscript

NIH-PA Author Manuscript

of mitochondrial permeability transition pore. Moreover, we hypothesized that cardiac-specific deletion of NMDA played an unrecognized role in cardiomyocyte mitophagy induction and regulation.

Materials and methods

Generation of cardiac-specific knockout mice of NMDA-R1 gene

Because the homozygous deletion of NMDA-R1 was embryonic lethal, cardiac-specific deletion of NMDA-R1 was created. As described earlier (30), a breeding pairs of heterozygous mice with floxed targeted *NR1* gene [B6.129S4-Grin1^{tm2Stl}/J (NR1$^{fl/fl}$)] and heterozygous mice with α-myosin heavy chain (MHC) Cre transgenic [B6.129-Tg (Myh6-cre/Esr1)1Jmk/J (α-MHC-Cre)] were obtained from the Jackson laboratory (Bar Harbor, ME, USA). The mice heterozygous for floxed NMDA-R1 allele (NR1$^{fl/+}$) were bred to homozygosity (NR1$^{fl/fl}$) with no birth defects and were healthy until adulthood (4 weeks). These were then bred with α-MHC Cre transgenic mice to generate the mice homozygous for floxed NMDA-R1 allele, carrying the homozygous α-MHC Cre transgene (NR1$^{fl/fl}$; Cre^{+}). This breeding also produced the following littermates: NR1$^{fl/fl}$, NR1$^{fl/+}$, and Cre^{+} (genetic controls). At 5 weeks of age, mice from the four genotypes were given tamoxifen intraperitoneally (20 mg/kg body weight, dissolved at the final concentration of 4 mg/mL in 30% of ethanol-sterile PBS) or vehicle daily for 5 days. To demonstrate the Cre-directed excision of *NR1* gene, Western blot and confocal imaging were conducted for NMDA-R1 subunit in the isolated cardiomyocytes. Hyperhomocysteinemia (HHcy) was induced in the mice by administering 1.8 g of DL-Hcy/L in the drinking water for 6 weeks. The following treatment groups used were wild type (WT), WT + Hcy, NR1$^{fl/fl}$/Cre + Hcy, and the genetic control for NR1$^{fl/fl}$/Cre(NR1$^{fl/fl}$). MMP-9 knock-out (KO) mice were obtained from Jackson laboratories. Animal experiments were carried out according to the protocols approved by the Institutional Animal Care and Use Committee of the University of Louisville.

Adult ventricular myocyte isolation

Single ventricular myocytes from the adult mice heart were isolated according to the protocol as described elsewhere (17). Briefly, hearts from 8-week to 10-week-old mice were removed rapidly and perfused with calcium-free perfusion buffer (in mmol/L: 120.4 NaCl, 14.7 KCl, 1.2 $MgSO_4 \cdot H_2O$, 0.6 Na_2HPO_4, 0.6 KH_2PO_4, 10 Na-HEPES, 4.6 $NaHCO_3$, 30 taurine, 10 glucose, and 10 butanedione monoxime, pH 7.4) and then with the same buffer with added Liberase Bledzyme 4 (0.9 mg/mL) (Roche Applied Science, Indianapolis, IN, USA) for 15–20 min. Ventricles were removed and resuspended in perfusion buffer with 10% serum, and 1.25 μmol/L calcium was added to stop the digestion. Calcium was reintroduced into cells and was maintained at room temperature in Hanks' buffer (5.6 mmol/L D-glucose and 1.25 μmol/L calcium). Cell yield was ~50–70% with ~75–80% viability. There was no notable difference of yield between WT and cardiac-specific NMDA-R1 KO mice.

Confocal microscopy

Isolated cardiomyocytes were washed two times with the incubation buffer (in mmol/L): 120.4 NaCl, 14.7 KCl, 1.2 $MgSO_4 \cdot H_2O$, 0.6 Na_2HPO_4, 0.6 KH_2PO_4, and 10 Na-HEPES, pH 7.4. The cells were fixed in 3.7% paraformaldehyde in PBS for 30 min at room temperature. Cells were washed and permeabilized with 0.1% Triton X-100 for 20 min. After being washed, the myocytes were incubated with primary anti-MMP-9 antibody (Sigma) (1:500 dilution, prepared in 0.02% Tween 20/PBS) overnight at 4°C. Cells were washed, and goat anti-mouse fluorescein isothiocyanate (FITC)-conjugated secondary antibody (molecular probe) (1:500 dilution, prepared in PBS) was applied for 3 h at room temperature. Cells were washed and incubated with 50 ng/mL Mitotracker Red in the dark for 25 min. After

NIH-PA Author Manuscript

NIH-PA Author Manuscript

NIH-PA Author Manuscript

additional washes with PBS to remove unbound Mitotracker, the cells were mounted on the glass slides. The images were acquired using a laser confocal microscope (FluoView 1000). To enable the comparison of changes in fluorescence intensity and punctuate staining pattern, the images were acquired under the identical set of conditions. FITC fluorescence was imaged using a band pass filter set at 488 nm excitation and 510–540 nm emission. Mitotracker Red was imaged using a He-Ne laser (excitation 579 nm and emission 599 nm).

Cardiac mitochondria isolation

Cardiac mitochondria were isolated from following groups: WT, WT + Hcy, $NR1^{fl/fl}$/Cre + Hcy, genetic control mice $NR1^{fl/fl}$/Cre. The heart was quickly excised and washed in buffer containing 250 mM sucrose, 10 mM Tris, 1 mM EGTA, and pH 7.4 at 4°C. After changes of buffer, the cardiac samples were cut into small pieces and homogenized. The samples were centrifuged at 3000 *g* for 3 min to remove debris, and mitochondria were obtained by a differential centrifugation technique (31). All isolated mitochondria were kept on ice. The mitochondrial sub-fractions were tested for specific markers for HSP-60 for mitochondria and calpain-1 for cytosolic fractions. The isolated mitochondrial pellet was used for Western blot and in-gel gelatin zymography.

Measurement of the mitochondrial permeability transition

Mitochondrial swelling was determined by a decrease in light absorption at 540 nm with 250 μg of mitochondrial protein in swelling buffer containing: 250 mM sucrose, 10 mM Tris–Mops (pH 7.4), 1 mM KH_2PO_4, and 0.05 μM EGTA supplemented with 2 μM rotenone and 5 mM succinate by the method described elsewhere (32). The MPT was measured using JC-1 red fluorescent dye before and after the addition of $CaCl_2$ (250 μmol/L).

Mitochondrial respiration

Oxygen consumption of isolated mitochondria under various conditions was measured using the BD Oxygen Biosensor System as described previously (Wang et al, 2005). Mitochondria (1 mg) was resuspended in respiratory buffer [130 mM sucrose, 50 mM KCl, 5 mM $MgCl_2$, 5 mM KH_2PO_4, 50 μM EDTA, and 5 mM HEPES (pH 7.4) and 2 μM rotenone] in separate wells of the BD Oxygen Biosensor System Plate. Oxygen consumption was measured in a fluorescence plate reader at 485 nm excitation and 630 nm emission. Fluorescence values for each well were normalized to their value and then to the values of no-mitochondria controls at each time point.

Immunoblotting

Western blotting was performed as described earlier (33). Briefly, 15 μg mitochondria lysate protein was loaded onto 10–15% SDS–PAGE gels and electrophoresis under non-reducing conditions and then transferred on to nitrocellulose membranes. The membranes were blocked with 5% non-fat dry milk in TBS-T (50 mM Tris–HCl, 150 mM NaCl, 0.1% Tween 20, pH 7.4), incubated with respective primary antibodies for 1 h at room temperature. After probing with appropriate secondary antibodies for 1 h at room temperature the blots were developed using X-ray film (RPI Corp, Inc., Mount Prospect, IL, USA) with a Kodak 2000A developer (Eastman Kodak, Rochester, NY, USA). Image analysis was performed using UMAX PowerLock II (Taiwan). CoxIV was used as a loading control for mitochondria fraction and GAPDH for cytosolic fraction.

Mitochondrial MMP activity by in-gel gelatin zymography

Cardiac mitochondrial pellet was incubated overnight in MMP extraction buffer containing cacodylic acid (10 mmol/L), NaCl (0.15 mol/L), $ZnCl_2$ (20 mmol/L), NaN_3 (1.5 mmol/L), and 0.01% Triton X-100 (pH 5.0). Protein concentration was determined and the 60 μg

NIH-PA Author Manuscript

NIH-PA Author Manuscript

NIH-PA Author Manuscript

mitochondrial protein was electrophoresed on 7.5% non-reducing SDS–PAGE gels containing 2 mg/mL gelatin as a substrate at constant voltage. After electrophoresis, the gels were rinsed in renaturation buffer (2.5% Triton X-100) on a shaker for 30 min to remove SDS and were incubated overnight at 37°C in a water bath in activation buffer composed of (in mM) 50 Tris–HCl, pH 7.4, and 5 $CaCl_2$. Gels were stained using 0.5% Coomassie blue R-250 for 2 h, followed by appropriate destaining. MMP activity was detected as a white band on a dark blue background and quantified densitometrically using Un-Scan software (Silk Scientific, Orem, UT, USA).

Quantitative real-time PCR (QRT-PCR)

RNA isolation and QRT-PCR were performed to measure the mRNA level of MMP-9 using a method as described earlier (33).

Measurement of homocysteine

The level of Hcy was quantitatively analyzed with HPLC as described earlier (34).

Measurement of mitochondrial ROS production by MitoSox

A mitochondrion-specific hydroethidine-derivative fluorescent dye (Wang et al., 2005) was used to assess mitochondrial O_2 production in mitochondria. In brief, isolated myocytes were loaded with MitoSox (5 μM at 37°C for 10 min). After incubation, myocytes were washed and incubated with 200 nmol mitotracker-green (mitochondria marker) and 0.1 μmol/L DAPI for 20 min. Myocytes were washed twice and fixed in 4% paraformaldehyde after incubation. Images were captured by laser confocal microscope (FluoView 1000) and ImagePro image analysis software (Media Cybernetics, Silver Spring, MD, USA).

Measurement of $ONOO^-$ production

Intracellular $ONOO^-$ was monitored by labeling with dihydrorhodamine-123 (DHR-123) (35). Cardiomyocytes seeded on glass cover slips were incubated at 22°C for 30 min in DMEM containing a 10 μM of DHR-123 (Invitrogen, Carlsbad, CA, USA). After loading, myocytes were rinsed three times with DMEM and then placed on the stage of a Laser confocal microscope (Fluor View 1000). The $ONOO^-$ fluorescence was measured using excitation and emission wavelengths of 488 nm and 520 nm, respectively.

Statistical analysis

Each data set of biochemical experiments was analyzed using 4–6 hearts. Data obtained from the same myocyte were used to express results in terms of the percentage change relative to control (before treatment) for pooling for statistical analysis. Experiments using commercial biochemical assays were performed in triplicate. Values were presented as average ± SD. Statistical significance ($P < 0.05$) was determined by Student's *t*-test for two groups. One-way or two-way ANOVA was used to compare the respective data with WT, $NR1^{fl/fl}$/Cre + $NR1^{fl/fl}$/Cre^+, and $NR1^{fl/fl}$ with or without Hcy treatment according to the Bonferroni correction.

Results

Hcy-induced oxidative and nitrosative stresses in the myocyte mitochondria by agonizing NMDA-R1

The plasma levels of Hcy were 1.5 ± 0.55 μmol/L in control ($n = 5$). The levels of Hcy were increased to 20 ± 0.5 μmol/L ($n = 6$) following 6 weeks of Hcy administration. We found a significant increase in mitochondrial super-oxide generation in myocytes from hyperhomocysteinemic mice compared with WT mice. Interestingly, the cardiac-specific

NIH-PA Author Manuscript

NIH-PA Author Manuscript

NIH-PA Author Manuscript

deletion of NMDA-R1 mitigated the Hcy-induced increase in mitochondrial superoxide production (Figure 1). Mitochondrial nitrosative stress was measured by labeling with dihydrorhodamine-123, an $ONOO^-$ specific dye. We observed that Hcy-induced peroxinitrite generation in the mitochondria of myocyte. Interestingly, the deletion of NMDA-R1 ameliorated the mitochondrial peroxinitrite generation by Hcy (Figure 2). These results suggested that Hcy increased superoxide production and caused an increase in peroxinitrite generation in mitochondria of myocytes and cardiac-specific deletion of NMDA-R1 mitigated these increases.

To determine the mitochondrial viability, function, and respiration, the myocyte mitochondrial fractions were isolated and checked for their purity by using Western blot analysis (Figure 3A). Hcy induced the mitochondrial permeability transition pore by agonizing NMDA-R1. Interestingly, the Hcy-induced increase in MPT was attenuated by cardiac-specific deletion of NMDA-R1 (Figure 3B). This finding suggested that Hcy agonized NMDA-R1 and induced MPT.

Oxygen consumption

Alternation in MPT can alter the rate of oxygen consumption. We measured oxygen consumption using BD Biosciences oxygen Biosensor System. The entire plate was pre blanked and then mitochondria were seeded into the plate. As shown in Figure 3C, Hcy treatment decreased the oxygen consumption. Importantly, the Hcy-mediated decrease in oxygen consumption was mitigated by cardiac-specific deletion of NMDA-R1 (Figure 3C). This finding suggested that Hcy agonized NMDA-R1 and decreased the oxygen consumption rate in the mitochondria.

Cardiac-specific deletion of NMDA-R1 attenuated Hcy-induced mtMMP-9 in the myocyte mitochondria

Because oxidative and nitrosative stresses induced MMP activation, we determined whether Hcy activated intracellular MMP-9 via agonizing NMDA-R1 in isolated mitochondria. The production of MMP-9 in myocyte mitochondria was measured by in-gel-gelatin zymography and semiquantitative RT-PCR methods. As shown in Figure 4, Hcy induced the MMP-9 production in hyperhomocysteinemic myocytes compared with WT. Furthermore, Hcy-induced MMP-9 activation was ablated by cardiac-specific deletion of NMDA-R1. Consistent with gelatin zymography data, the transcript levels of MMP-9 were found to be significantly lower in $NR1^{fl/fl}$/Cre($NR1^{fl/f}$) mice compared with $NR1^{fl/fl}$/Cre($NR1^{fl/f}$) + Hcy (Figure 4B). This suggested that Hcy activated MMP-9 in the myocyte mitochondria by agonizing NMDA-R1.

Effect of Hcy on mitochondrial connexin-43

To determine whether Hcy induced translocation to mitochondria and degradation of Cxn-43, connexin-43, and mitochondria were co-localized (Figure 5), suggesting connexin-43 translocation during HHcy. In mice with cardiac-specific deletion of NMDA-R1, the localization of connexin-43 was inhibited (Figure 5). These results suggested that Hcy induced disarray and translocation of connexin-43, and deletion of NMDA-R1 mitigated this translocation.

Deletions of NMDA-R1 and MMP-9 decreased mitochondrial connexin-43 degradation

To determine connexin-43 degradation, we performed western blot analysis on isolated mitochondria and observed that Cxn-43 was localized in the mitochondrial membrane fraction. More interestingly, we observed that Hcy treatment induced degradation of mtCxn-43 (Figure 6). Furthermore, deletions of NMDA-R1 or MMP-9 genes mitigated the

NIH-PA Author Manuscript

NIH-PA Author Manuscript

NIH-PA Author Manuscript

degradation. This suggested that Cxn-43 was a novel MMP-9 target and Hcy-induced mtCxn-43 degradation, causing mitochondrial permeability transition pore.

Hcy-induced mitochondrial mitophagy in cardiomyocytes

The conversion of LC3-I to LC3-II was an indicator of autophagy activation, in mitochondria it was mitophagy. The mitophagy was assessed by immunoblot analysis using LC3 antibody (Figure 7). LC3-II abundance increased by Hcy. Cardiac-specific deletion of NMDA-R1 inhibited the conversion of LC3-II (Figure 7). Interestingly, the MMP-9 KO also mitigated the LC3-II generation. These results suggested that Hcy induced mitophagy, in part, by activation MMP-9 and NMDA-R1.

Discussion

Previously we have shown that HHcy induced ROS and NO production, as well as mitochondrial permeability transition (MPT). These effects were blocked by pharmacological inhibitors of NMDA-R1 (11,17). Here we have presented the new data relating HHcy to NMDA-R1 and mitochondria mitophagy. In Figure 7, the data showed that NMDA-R1 deletion decreased the expression of LC3-I. In Figure 6, the data showed that NMDA-R1 deletion decreased the degradation of mtCxn-43. In addition, we demonstrated that MMP-9 KO mitigated not only degradation of Cxn-43 but also increased LC3-II, a marker of autophagy/mitophagy.

The apparent reduction in MMP-9 mitochondrial translocation in myocyte-specific NMDA-R1 KO mice in the presence of HHcy may be secondary to reduced MMP-9 expression. However, we demonstrated that in MMP-9 KO mice Hcy treatment has less effect. Previously, we have shown that Hcy induced mitochondrial oxidative stress and activated MMP-9 by agonizing NMDA-R1 (30). Although there was less mitigation in the mRNA levels of MMP-9 after Hcy treatment (Figure 4C and 4D), the cardiac-specific deletion of NMDA-R1 gene mitigated the MMP-9 activation in gelatin-gel zymography (Figure 4A and 4B).

To demonstrate the functional relevance of connexin-43 mitochondrial “localization” and “degradation”, we showed that MMP-9 KO mitigated the localization and degradation of Cxn-43. Hcy caused an increase in oxidative and nitrosative stresses, including nitrogen free radical generation in the myocyte mitochondria and the activation of MMP. The activation of MMP-9 induced connexin-43 (Cxn-43) translocation to mitochondria, leading to cardiomyocyte mitophagy. These effects of Hcy were ameliorated by cardiac-specific ablation of NMDA-R1 or MMP-9 gene deletion. These observations unequivocally supported the notion that high Hcy activated MMP-9 in the myocyte mitochondria and degraded gap junction protein connexin-43, leading to mitophagy, in part, by agonizing NMDA-R1.

The fluorescence in the panel of Figure 5 is weak. However, we have confirmed the conclusion in several lines of experiments. We have demonstrated that significant levels of connexin-43 were present in isolated mitochondrial fractions from Hcy-treated animals as compared with untreated animals (Figure 6). Interestingly, in MMP-9−/−, the translocation and degradation of connexin-43 by Hcy treatment was mitigated (Figure 7). The fluorescence images were just to further support the results from gel experiments in isolated mitochondrial fractions. Others have shown that Hcy-mediated the translocation of connexin-43 to the mitochondria (22).

Whether proMMP-9 or active MMP-9 was responsible for the degradation of connnexin was not addressed. However, active MMP-9 was most probably responsible for Cxn-43

NIH-PA Author Manuscript

NIH-PA Author Manuscript

NIH-PA Author Manuscript

degradation, because most of the MMPs in the myocardium were in latency due to the co-ordination of zinc ion with constitutive nitric oxide in the ternary complex (MMP–NO–TIMP) in the basement membrane. The latent MMPs were activated during increase in oxidative stress (36).

Oxidative stress plays an important role in various pathological conditions, such as cardiac disease, which has been demonstrated to be autophagy related (37). However, the role of autophagy under those conditions was controversial. Hcy induced oxidative stress, mainly by the upregulation of the superoxide-producing enzyme, NADPH oxidase (38). A major reaction of superoxide was with NO to form the potent oxidant, peroxynitrite (38). It has been reported that Hcy also induced apoptosis (39,40) or autophagy (41). In this study, we have demonstrated that HHcy induced mitophagy/autophagy in cardiomyocytes through cardiac-specific NMDA-R1 receptor.

In the present study, we have reported that HHcy induced the generation of mitochondrial ROS and per-oxinitrite in the mitochondria of myocyte by agonizing the NMDA-R1. We presented the evidence that cardiac-specific deletion of NMDA-R1 caused a decrease in Hcy-induced MMP-9 activation in the myocyte mitochondria. This was consistent with our earlier finding that Hcy agonized NMDA-R1 and caused MPT by MMP activation (17). Homocysteine-mediated ROS production may not be related to Hcy-mediated NMDA-R1 stimulation. However, it was known that Hcy acted as agonist to NMDA-R1. The activation of NMDA-R1 increased ROS production and, therefore, damaged the mitochondria leading apoptosis in neonatal cardiomyocytes (42).

Normally mitochondrial connexin-43 was fully phosphorylated, but it was dephosphorylated for example during ischemia. The data in Figure 6A could be interpreted as increased dephosphorylation of connexin-43 in HHcy. However, we have verified that connexin-43 was degraded rather than dephosphorylated using MMP-9 KO myocytes (Figure 6B). Cxn-43 was a novel target for MMP and abundantly expressed in cardiomyocytes. However, the functional consequences of Cxn-43 translocation were not well understood. In the present study, we have reported that Hcy down-regulated Cxn-43 in the membrane fraction of cardiac mitochondria. Cardiac-specific ablations of NMDA-R1 ameliorated Hcy-induced increase of mtMMP-9 expression and resulted in the down-regulation of mtCxn-43. Furthermore, there were measurable increases in mitochondrial oxidative stress as well as activation of mtMMP with the degradation of mtCxn-43. This led to contractile and electrical dysfunction in cardiomyocytes, in part, by opening mitochondrial permeability transition pores and releasing mitophagy inducing factor. Our results indicated that mitophagy occurred with an increase in the protein level of LC3-II and degradation of Cxn-43. Cardiomyocyte mitophagy was inhibited by cardiac-specific deletion of NMDA receptor and MMP-9 deletion.

In conclusion, our study revealed that cardiomyocyte-specific deletion of NMDA-R1 incited the following results: mitigation of Hcy-induced myocyte mitochondrial ROS, mitigation of NO levels, activation of MMP-9, and nitrosylation of Cxn-43 in the cardiac mitochondria. Furthermore, activated mtMMP-9 caused mtCxn-43 degradation that led to mitophagy (Figure 8). Mitochondria were among the most important targets of oxidative stress; therefore, future studies will be directed toward understanding the function of the membrane channels, mitochondrial proteins, or genes targeted to mitochondria, in order to further elucidate the mechanisms of mitophagy.

Limitations

The data were presented to link MMP-9 with LC3-I cleavage. However, it was possible that other proteases such as the ROS-activated protease Atg4B were involved in the conversion

NIH-PA Author Manuscript

NIH-PA Author Manuscript

NIH-PA Author Manuscript

of LC3-I to LC3-II (43). Also our data implied that mitochondrial autophagy was always detrimental to the cell; however, it has been shown that mitophagy may be a targeted defense against oxidative stress by removing damaged mitochondria. Therefore, mitophagy can be beneficial or detrimental depending on the levels of pathogenesis.

The functional consequence and/or importance of increased autophagy/mitophagy in the mitochondria of cardiac cells needs more proof: (1) the contractility of the cardiac cells obtained from various groups of animals should be assessed/measured. (2) Some of the previous studies indicated that HHcy elicited increase in systemic blood pressure. Therefore, the blood pressure of animals of various groups should be measured. (3) The heart rate of animals of various groups should be measured, especially because we previously demonstrated the importance of arrhythmia induced by HHcy. These studies are in progress.

Acknowledgments

A part of this study was supported by NIH grants: HL-71010, HL-74185, and HL-88012.

References

1. Scott JM, Weir DG. Folic acid, homocysteine and one-carbon metabolism: a review of the essential biochemistry. J Cardiovasc Risk 1998;5:223–227. [PubMed: 9919469]
2. Folbergrová J. NMDA and not non-NMDA receptor antagonists are protective against seizures induced by homocysteine in neonatal rats. Exp Neurol 1994;130:344–350. [PubMed: 7867764]
3. Lipton SA, Kim WK, Choi YB, et al. Neurotoxicity associated with dual actions of homocysteine at the N-methyl-D-aspartate receptor. Proc Natl Acad Sci USA 1997;94:5923–5928. [PubMed: 9159176]
4. Lalo U, Pankratov Y, Kirchhoff F, North RA, Verkhratsky A. NMDA receptors mediate neuron-to-glia signaling in mouse cortical astrocytes. J Neurosci 2006;26:2673–2683. [PubMed: 16525046]
5. Krainc D, Bai G, Okamoto S, et al. Synergistic activation of the N-methyl-D-aspartate receptor subunit 1 promoter by myocyte enhancer factor 2C and Sp1. J Biol Chem 1998;273:26218–26224. [PubMed: 9748305]
6. Qureshi I, Chen H, Brown AT, et al. Homocysteine-induced vascular dysregulation is mediated by the NMDA receptor. Vasc Med 2005;10:215–223. [PubMed: 16235775]
7. Duchen MR. Mitochondria in health and disease: perspectives on a new mitochondrial biology. Mol Aspects Med 2004;25:365–451. [PubMed: 15302203]
8. DiMicco J, Monroe AJ. Stimulation of metabotropic glutamate receptors in the dorsomedial hypothalamus elevates heart rate in rats. Am J Physiol 1996;270:R1115–R1121. [PubMed: 8928914]
9. Moshal KS, Singh M, Sen U, et al. Homocysteine-mediated activation and mitochondrial translocation of calpain regulates MMP-9 in MVEC. Am J Physiol Heart Circ Physiol 2006;291:H2825–H2835. [PubMed: 16877562]
10. Frey U, Müller M, Kuhl D. A different form of long-lasting potentiation revealed in tissue plasminogen activator mutant mice. J Neurosci 1996;16:2057–2063. [PubMed: 8604050]
11. Mihm MJ, Yu F, Carnes CA, et al. Impaired myofibrillar energetics and oxidative injury during human atrial fibrillation. Circulation 2001;104:174–180. [PubMed: 11447082]
12. Rosenberg GA. Matrix metalloproteinases in neuroinflammation. Glia 2002;39:279–291. [PubMed: 12203394]
13. Tyagi N, Sedoris KC, Steed M, Ovechkin AV, Moshal KS, Tyagi SC. Mechanisms of homocysteine-induced oxidative stress. Am J Physiol Heart Circ Physiol 2005;289:H2649–H2656. [PubMed: 16085680]
14. Rucklidge GJ, Milne G, McGaw BA, Milne E, Robins SP. Turnover rates of different collagen types measured by isotope ratio mass spectrometry. Biochim Biophys Acta 1992;1156:57–61. [PubMed: 1472539]

NIH-PA Author Manuscript

NIH-PA Author Manuscript

NIH-PA Author Manuscript

15. Sood HS, Cox MJ, Tyagi SC. Generation of nitrotyrosine precedes activation of metalloproteinase in myocardium of hyperhomocysteinemic rats. Antioxid Redox Signal 2002;4:799–804. [PubMed: 12470508]
16. Limb GA, Matter K, Murphy G, et al. Matrix metalloproteinase-1 associates with intracellular organelles and confers resistance to lamin A/C degradation during apoptosis. Am J Pathol 2005;166:1555–1563. [PubMed: 15855654]
17. Moshal KS, Tipparaju SM, Vacek TP, et al. Mitochondrial matrix metalloproteinase activation decreases myocyte contractility in hyperhomocysteinemia. Am J Physiol Heart Circ Physiol 2008;295:H890–H897. [PubMed: 18567713]
18. Heil SG, De Vriese AS, Kluijtmans LA, Mortier S, Den Heijer M, Blom HJ. The role of hyperhomocysteinemia in nitric oxide (NO) and endothelium-derived hyperpolarizing factor (EDHF)-mediated vasodilatation. Cell Mol Biol (Noisy-le-grand) 2004;50:911–916. [PubMed: 15704255]
19. Rosenberger D, Moshal KS, Kartha GK, et al. Arrhythmia and neuronal/endothelial myocyte uncoupling in hyperhomocysteinemia. Arch Physiol Biochem 2006;112:219–227. [PubMed: 17178594]
20. Jongsma HJ, Wilders R. Gap junctions in cardiovascular disease. Circ Res 2000;86:1193–1197. [PubMed: 10864907]
21. Kléber AG, Rudy Y. Basic mechanisms of cardiac impulse propagation and associated arrhythmias. Physiol Rev 2004;84:431–488. [PubMed: 15044680]
22. Li H, Brodsky S, Kumari S, et al. Paradoxical overexpression and translocation of connexin43 in homocysteine-treated endothelial cells. Am J Physiol Heart Circ Physiol 2002;282:H2124–H2133. [PubMed: 12003820]
23. Hunt MJ, Tyagi SC. Peroxisome proliferators compete and ameliorate Hcy-mediated endocardial endothelial cell activation. Am J Physiol, Cell Physiol 2002;283:C1073–C1079. [PubMed: 12225971]
24. Rodriguez-Sinovas A, Boengler K, Cabestrero A, et al. Translocation of connexin 43 to the inner mitochondrial membrane of cardiomyocytes through the heat shock protein 90-dependent TOM pathway and its importance for cardioprotection. Circ Res 2006;99:93–101. [PubMed: 16741159]
25. Lindsey ML, Escobar GP, Mukherjee R, et al. Matrix metalloproteinase-7 affects connexin-43 levels, electrical conduction, and survival after myocardial infarction. Circulation 2006;113:2919–2928. [PubMed: 16769909]
26. Lemasters JJ. Selective mitochondrial autophagy, or mitophagy, as a targeted defense against oxidative stress, mitochondrial dysfunction, and aging. Rejuvenation Res 2005;8:3–5. [PubMed: 15798367]
27. Nakai A, Yamaguchi O, Takeda T, et al. The role of autophagy in cardiomyocytes in the basal state and in response to hemodynamic stress. Nat Med 2007;13:619–624. [PubMed: 17450150]
28. Hickson-Bick DL, Jones C, Buja LM. Stimulation of mitochondrial biogenesis and autophagy by lipopolysaccharide in the neonatal rat cardiomyocyte protects against programmed cell death. J Mol Cell Cardiol 2008;44:411–418. [PubMed: 18062988]
29. Rothermel BA, Hill JA. Autophagy in load-induced heart disease. Circ Res 2008;103:1363–1369. [PubMed: 19059838]
30. Moshal KS, Kumar M, Tyagi N, et al. Restoration of contractility in hyperhomocysteinemia by cardiac-specific deletion of NMDA-R1. Am J Physiol Heart Circ Physiol 2009;296:H887–H892. [PubMed: 19181966]
31. Shiva S, Brookes PS, Darley-Usmar VM. Methods for measuring the regulation of respiration by nitric oxide. Methods Cell Biol 2007;80:395–416. [PubMed: 17445706]
32. Varela AT, Gomes AP, Simões AM, et al. Indirubin-3′-oxime impairs mitochondrial oxidative phosphorylation and prevents mitochondrial permeability transition induction. Toxicol Appl Pharmacol 2008;233:179–185. [PubMed: 18786556]
33. Tyagi N, Ovechkin AV, Lominadze D, Moshal KS, Tyagi SC. Mitochondrial mechanism of microvascular endothelial cells apoptosis in hyperhomocysteinemia. J Cell Biochem 2006;98:1150–1162. [PubMed: 16514665]

NIH-PA Author Manuscript

NIH-PA Author Manuscript

NIH-PA Author Manuscript

34. Sen U, Tyagi N, Kumar M, Moshal KS, Rodriguez WE, Tyagi SC. Cystathionine-beta-synthase gene transfer and 3-deazaadenosine ameliorate inflammatory response in endothelial cells. Am J Physiol, Cell Physiol 2007;293:C1779–C1787. [PubMed: 17855772]
35. Brahma MK, Dohare P, Varma S, et al. The neuronal apoptotic death in global cerebral ischemia in gerbil: important role for sodium channel modulator. J Neurosci Res 2009;87:1400–1411. [PubMed: 19115407]
36. Tyagi SC, Ratajska A, Weber KT. Myocardial matrix metalloproteinase(s): localization and activation. Mol Cell Biochem 1993;126:49–59. [PubMed: 8107689]
37. Lefer DJ, Granger DN. Oxidative stress and cardiac disease. Am J Med 2000;109:315–323. [PubMed: 10996583]
38. Levrand S, Pacher P, Pesse B, et al. Homocysteine induces cell death in H9C2 cardiomyocytes through the generation of peroxynitrite. Biochem Biophys Res Commun 2007;359:445–450. [PubMed: 17544363]
39. Tyagi N, Moshal KS, Ovechkin AV, et al. Mitochondrial mechanism of oxidative stress and systemic hypertension in hyperhomocysteinemia. J Cell Biochem 2005a;96:665–671. [PubMed: 16149054]
40. Sipkens JA, Krijnen PA, Meischl C, et al. Homocysteine affects cardiomyocyte viability: concentration-dependent effects on reversible flip-flop, apoptosis and necrosis. Apoptosis 2007;12:1407–1418. [PubMed: 17440815]
41. Dennis PB, Mercer CA. The GST-BHMT assay and related assays for autophagy. Meth Enzymol 2009;452:97–118. [PubMed: 19200878]
42. Gao X, Xu X, Pang J, et al. NMDA receptor activation induces mitochondrial dysfunction, oxidative stress and apoptosis in cultured neonatal rat cardiomyocytes. Physiol Res 2007;56:559–569. [PubMed: 16925458]
43. Scherz-Shouval R, Shvets E, Fass E, Shorer H, Gil L, Elazar Z. Reactive oxygen species are essential for autophagy and specifically regulate the activity of Atg4. EMBO J 2007;26:1749–1760. [PubMed: 17347651]
44. Wang W, Upshaw L, Strong DM, Robertson RP, Reems J. Increased oxygen consumption rates in response to high glucose detected by a novel oxygen biosensor system in non-human primate and human islets. J Endocrinol 2005 Jun;185(3):445–455. [PubMed: 15930171]

NIH-PA Author Manuscript

NIH-PA Author Manuscript

NIH-PA Author Manuscript

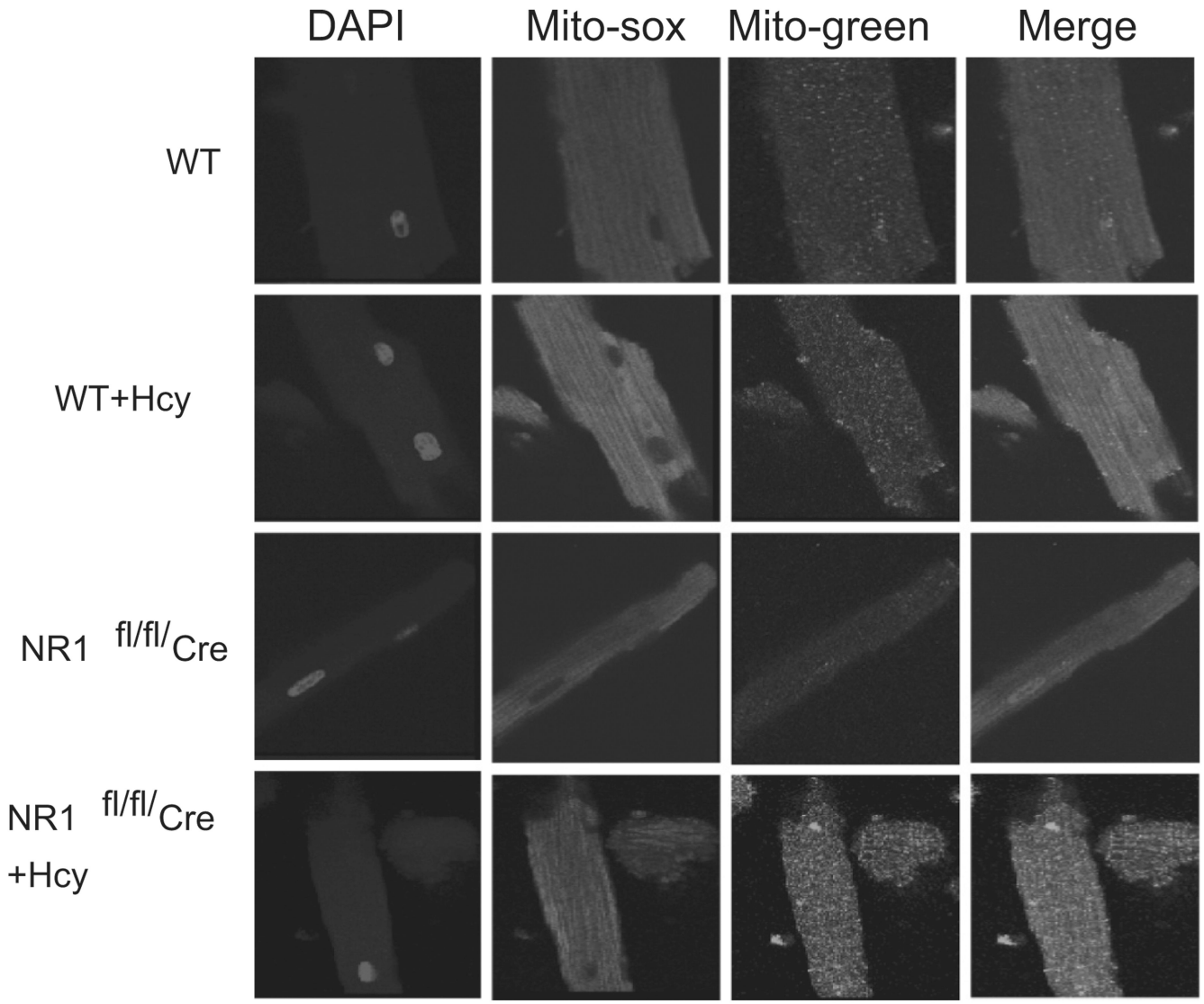

Figure 1.

In situ labeling of superoxide production in isolated adult ventricular myocyte by mito-sox stain: Myocytes were isolated from WT, WT + Hcy-treated for 6 weeks, NMDA-R1 knockout (NR1-KO)-treated with Hcy, and NR1-KO (control) mice. The images were captured by confocal microscope. The mito-Sox stain was used as a marker for superoxide radical generation. Mitotracker-green was used to identify the mitochondria. The DAPI stain was used for nuclear localization. All three images were merged. Magnification was ×20.

NIH-PA Author Manuscript
NIH-PA Author Manuscript
NIH-PA Author Manuscript

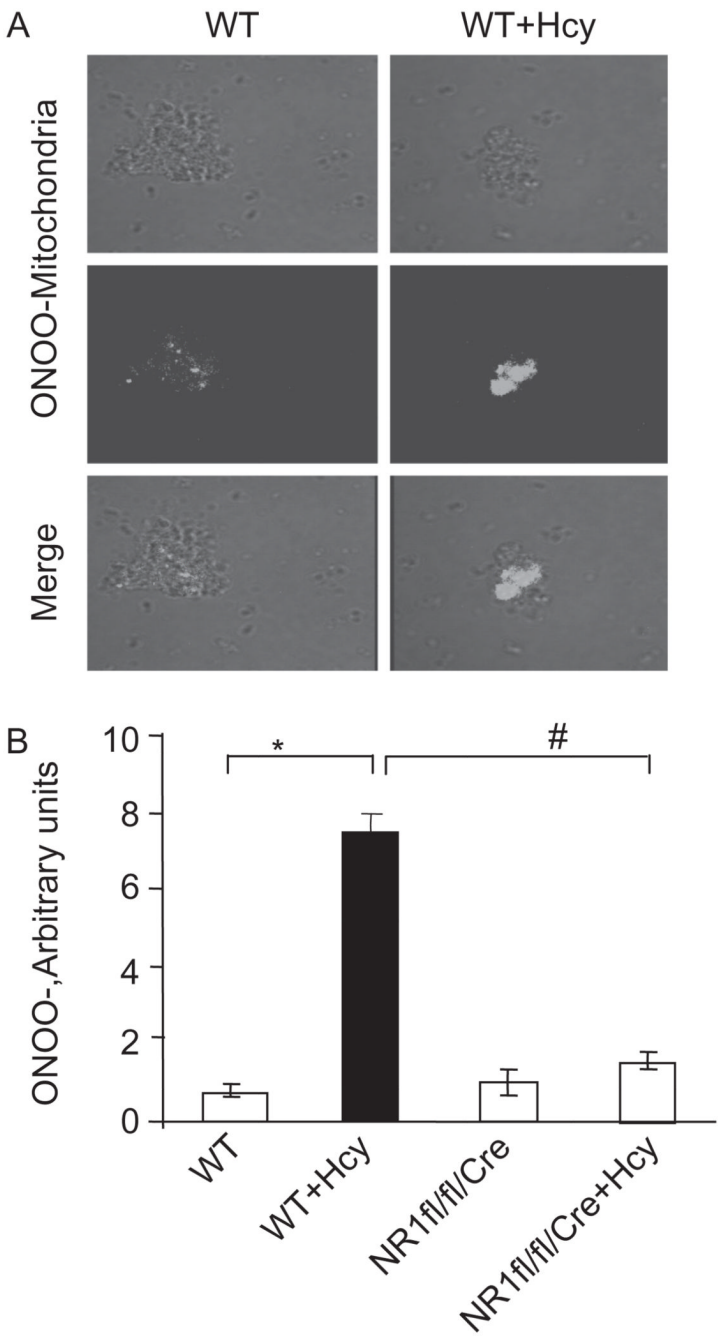

Figure 2.

(A) Mitochondria were isolated from myocytes from WT, WT + Hcy-treated for 6 weeks, NMDA-R1 knockout (NR1-KO)-treated with Hcy, and NR1-KO (control) mice. The light transmission micrograph of mitochondria and generation f peroxinitrite ($ONOO^{-}$) were detected by labeling with dihydrorhodamine 123 (DHR). The two panels were merged. (B) Densitometric analysis of mitochondrial $ONOO^{-}$ production was performed and plotted as a bar graph in arbitrary units. *$P < 0.05$ compared with WT; #$P < 0.05$ compared with $NR1^{fl/fl}$/Cre with Hcy. Data are the representative of four different experiments.

NIH-PA Author Manuscript
NIH-PA Author Manuscript
NIH-PA Author Manuscript

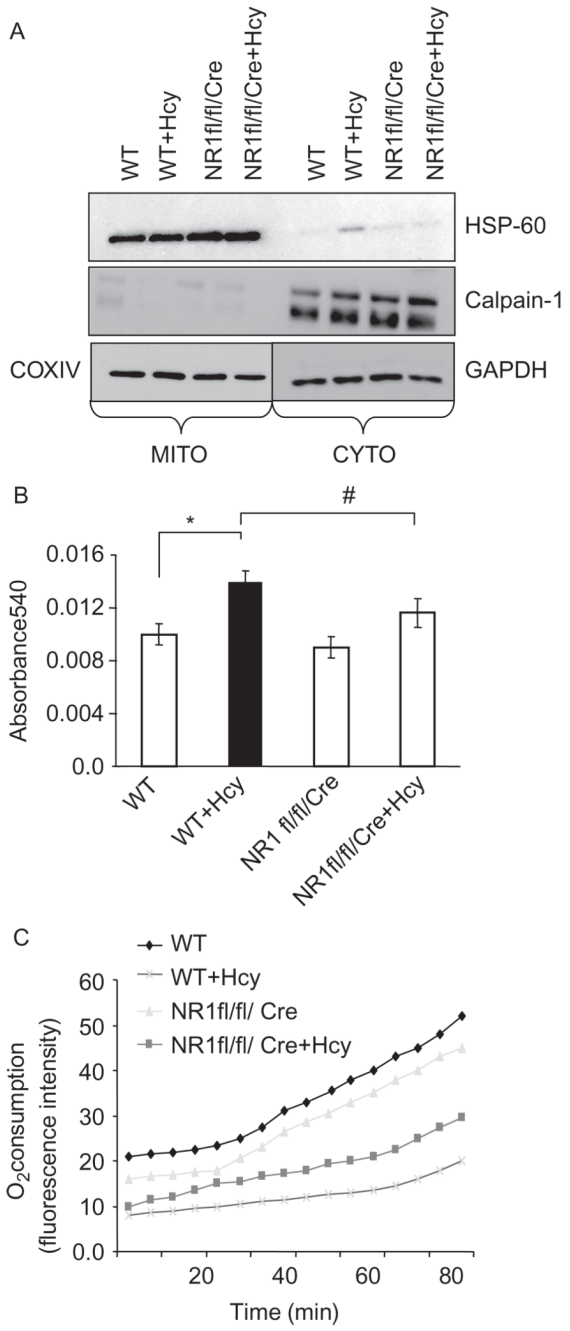

Figure 3.

(A) Isolation and characterization of mitochondria (MITO) and cytosolic (CYTO) fractions: myocytes from WT, WT + Hcy-treated for 6 weeks, NMDA-R1 knockout (NR1-KO)-treated with Hcy, and NR1-KO (control) mice were isolated and mitochondria were separated. Mitochondrial and cytosolic fractions were characterized by heat shock protein (HSP-60) in mitochondria and calpain-1 in the cytosol by western blot analysis. GAPDH was used as loading control for cytosol and COXIV for mitochondrial fractions. (B) Measurements of mitochondrial permeability transition (MPT) pore: the mitochondria from four groups were isolated and suspended in swelling buffer (pH7.4) $CaCl_2$ was added to initiate the swelling, and the absorbance was recorded at 540 nm (A_{540}). δA_{540} was

NIH-PA Author Manuscript

NIH-PA Author Manuscript

NIH-PA Author Manuscript

calculated and plotted. ($\delta A_{540} = A_{540max} - A_{540min}$). ($n = 4$ in each group). (C) Mitochondrial oxygen (O_2) consumption was measured by gradual increase in fluorescence at 630 nm when excited at 485 nm as mitochondrial capacity to utilize the oxygen using oxygen-sensitive fluorescent dye, tris(4,7-diphenyl-1,10 phenanthroline) ruthenium (II) chloride, embedded in a gas-permeable silicone polymer matrix affixed to each well bottom of a standard Falcon microplate (BD Oxygen Biosensor system). The change in fluorescence with time was measured.

NIH-PA Author Manuscript

NIH-PA Author Manuscript

NIH-PA Author Manuscript

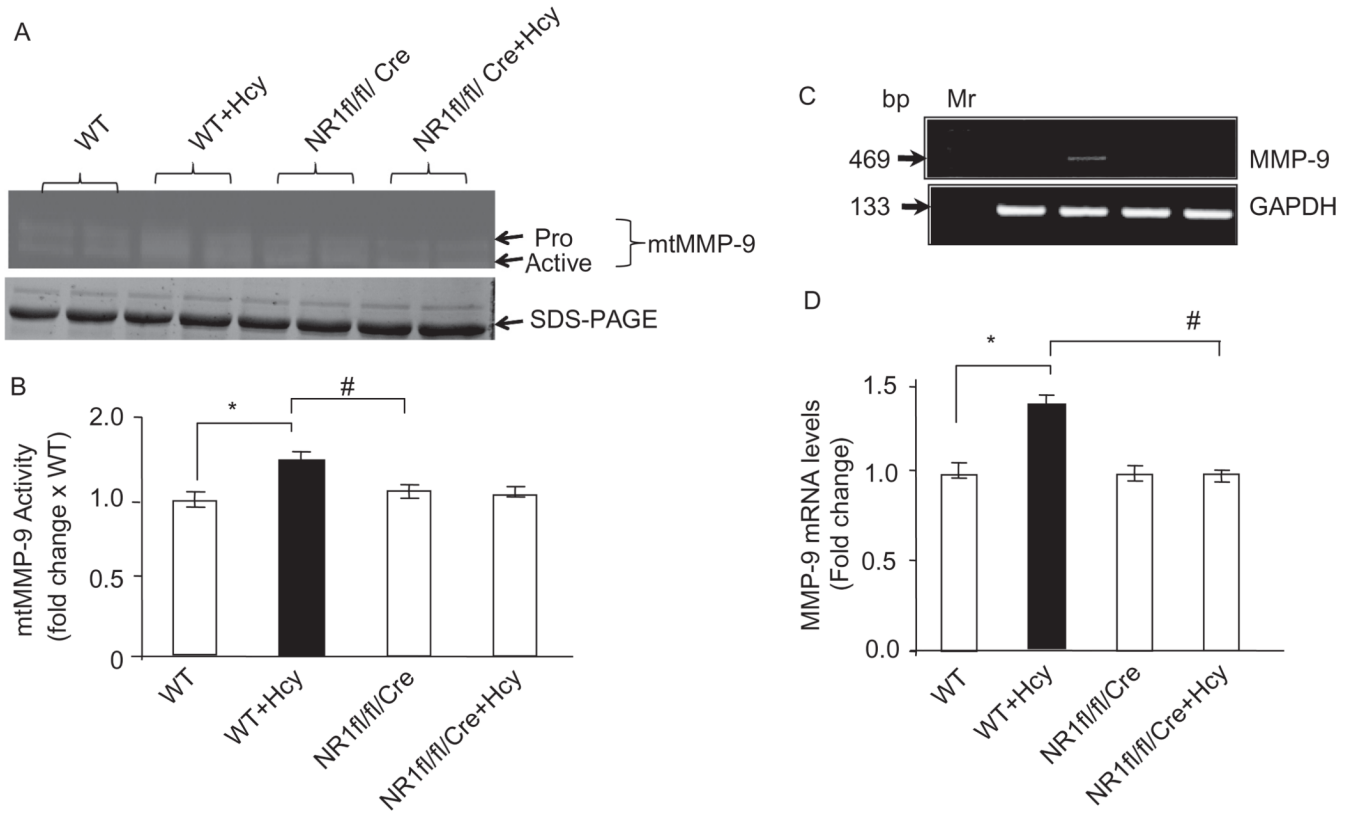

Figure 4.

(A) Cardiac-specific deletion of NMDA-R1 attenuates the Hcy-induced MMP-9 activity: cardiac mitochondria was isolated and processed for in-gel gelatin zymography. A representative zymogram is presented. (B) Densitometric analysis was performed and plotted as a bar graph as fold change to WT. *$P < 0.05$ compared with WT; #$P < 0.05$ compared with $NR1^{fl/fl}$/Cre with Hcy ($n = 4$ per group). (C) The levels of myocyte MMP-9 mRNA expression by RT-PCR in WT, WT + Hcy-treated for 6 weeks, NMDA-R1 knockout (NR1-KO)-treated with Hcy, and NR1-KO (control) mice. (D) The bands were scanned and fold increase in MMP-9 mRNA levels of NMDAKO + Hcy mice compared with control was presented. * $P < 0.05$ compared with WT; #$P < 0.05$ compared with $NR1^{fl/fl}$/Cre with Hcy ($n = 4$ in each group).

NIH-PA Author Manuscript
NIH-PA Author Manuscript
NIH-PA Author Manuscript

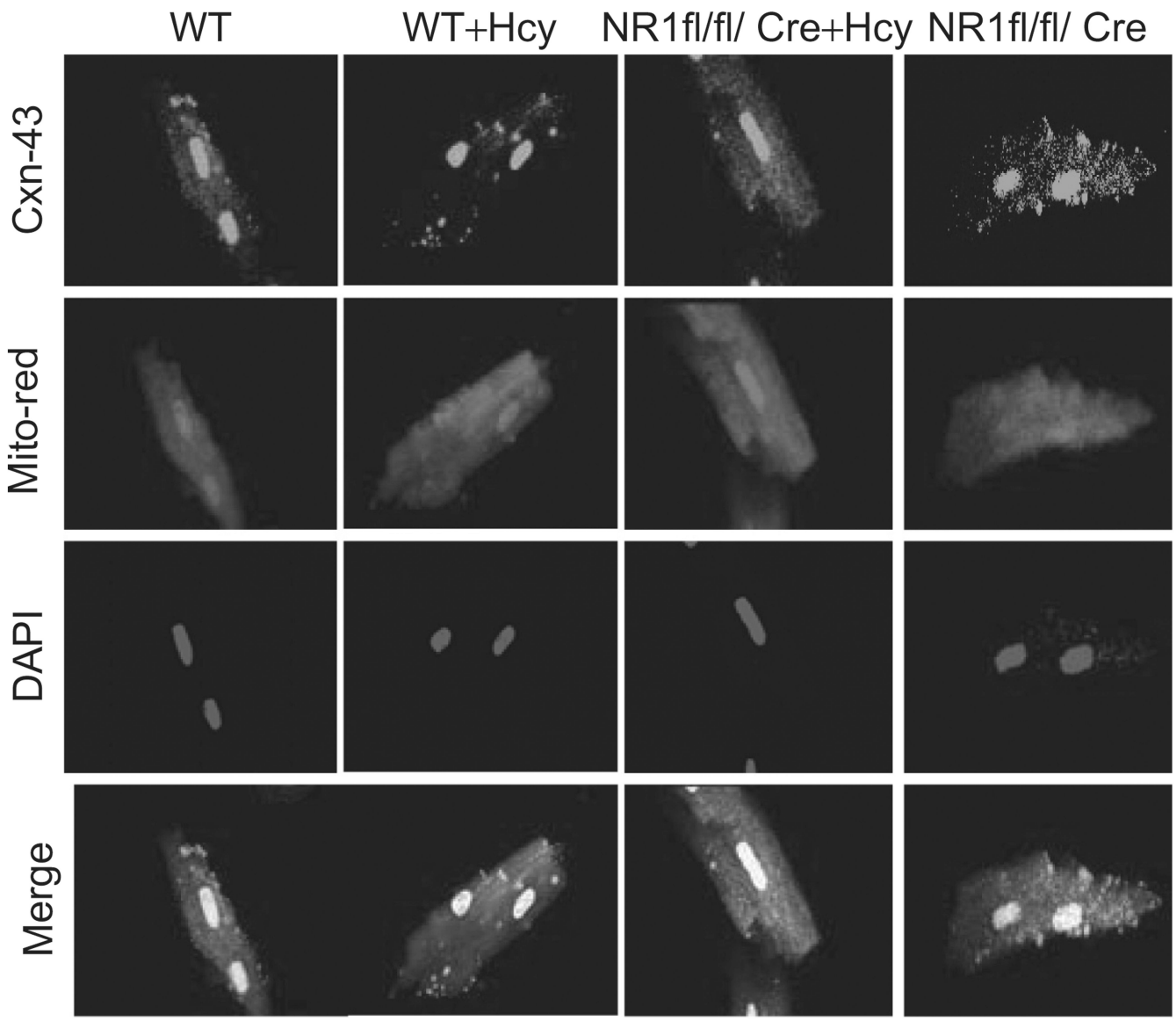

Figure 5.
Mitochondria and connexin-43 in NMDA-R1 deletion: the myocytes were isolated from WT, WT + Hcy-treated for 6 weeks, NMDA-R1 knockout (NR1-KO)-treated with Hcy, and NR1-KO (control) mice. The myocytes were labeled for connexin-43 (Cxn-43) antibody, mitrotacker-red (for mitochondia) and DAPI for nuclei. The merge panels were for Cxn-43, mitochondria, and nuclei.

NIH-PA Author Manuscript

NIH-PA Author Manuscript

NIH-PA Author Manuscript

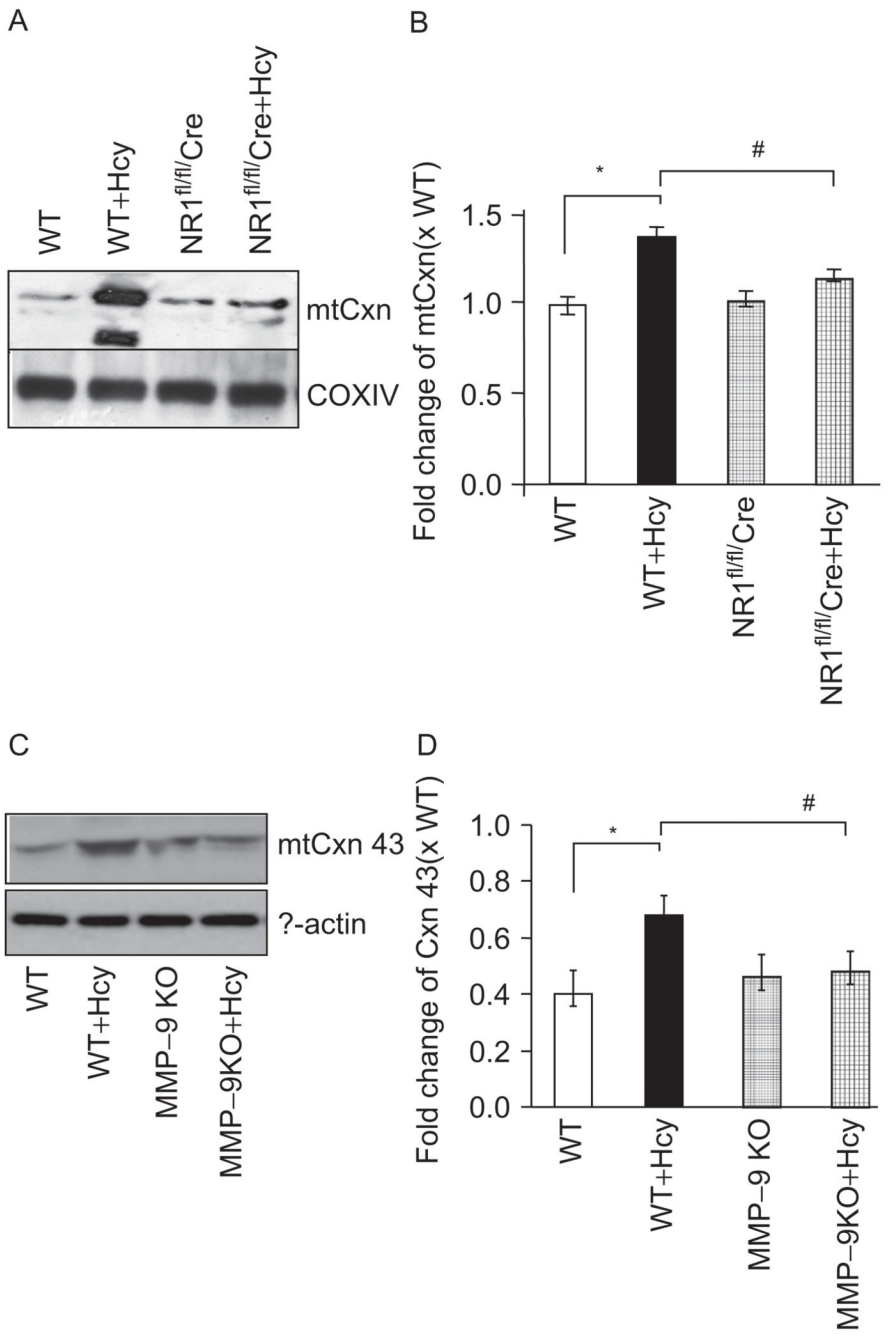

Figure 6.

Translocation of mtCxn-43: (A) immunobloting for Cxn-43 in mitochondrial fractions from WT, WT + Hcy-treated for 6 weeks, NMDA-R1 knockout (NR1-KO)-treated with Hcy, and NR1-KO (control) mice. The COXIV was used as control. (B) Densitometric analysis was performed and plotted as a bar graph. **P* < 0.05 compared with WT; #*P* < 0.05 compared with $NR1^{fl/fl}$/Cre with Hcy. Data were representative of *n* = 4 in each group. (C) Degradation of Cxn-43 was measured in myocytes from WT, WT + Hcy-treated for 6 weeks, MMP-9 knockout (MMP-9KO)-treated with Hcy, and MMP-9-KO (control) mice. The β-actin was used as control. (D) The bands were scanned and presented as bar graphs.

NIH-PA Author Manuscript

NIH-PA Author Manuscript

NIH-PA Author Manuscript

*$P < 0.05$ compared with WT; #$P < 0.05$ compared with MMP-9KO with Hcy. Data were representative of $n = 4$ in each group.

NIH-PA Author Manuscript

NIH-PA Author Manuscript

NIH-PA Author Manuscript

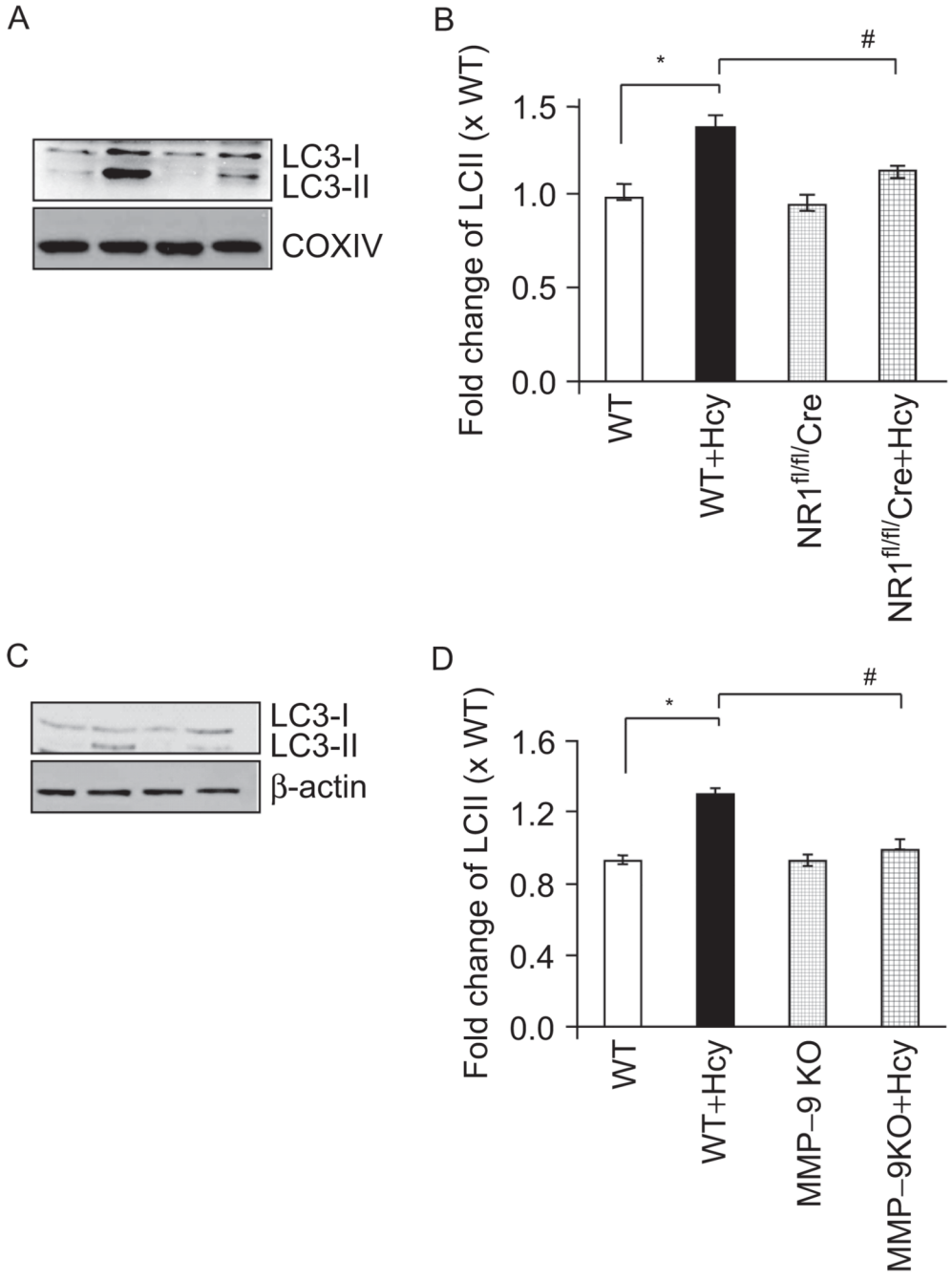

Figure 7.

Hcy-induced autophagy is partially abrogated by cardiac specific deletion of NMDA receptor. (A) Immunobloting for cleaved LC3 (LC3-II) using myocyte mitochondrial fractions from WT, WT + Hcy-treated for 6 weeks, NMDA-R1 knockout (NR1-KO)-treated with Hcy, and NR1-KO (control) mice. (B) Densitometric analysis was performed and plotted as a bar graph. **P* < 0.05 compared with WT; #*P* < 0.05 compared with $NR1^{fl/fl}$/Cre with Hcy. Data are the representative of *n* = 4 per group. (C) MMP-9 mediated LC3 degradation was measured in myocytes from WT, WT + Hcy-treated for 6 weeks, MMP-9 knockout (MMP-9KO)-treated with Hcy, and MMP-9KO (control) mice. The β-actin was used as control. (D) The bands were scanned and presented as bar graphs. **P* < 0.05

compared with WT; #$P < 0.05$ compared with MMP-9KO with Hcy. Data were representative of $n = 4$ in each group.

NIH-PA Author Manuscript

NIH-PA Author Manuscript

NIH-PA Author Manuscript

NIH-PA Author Manuscript
NIH-PA Author Manuscript
NIH-PA Author Manuscript

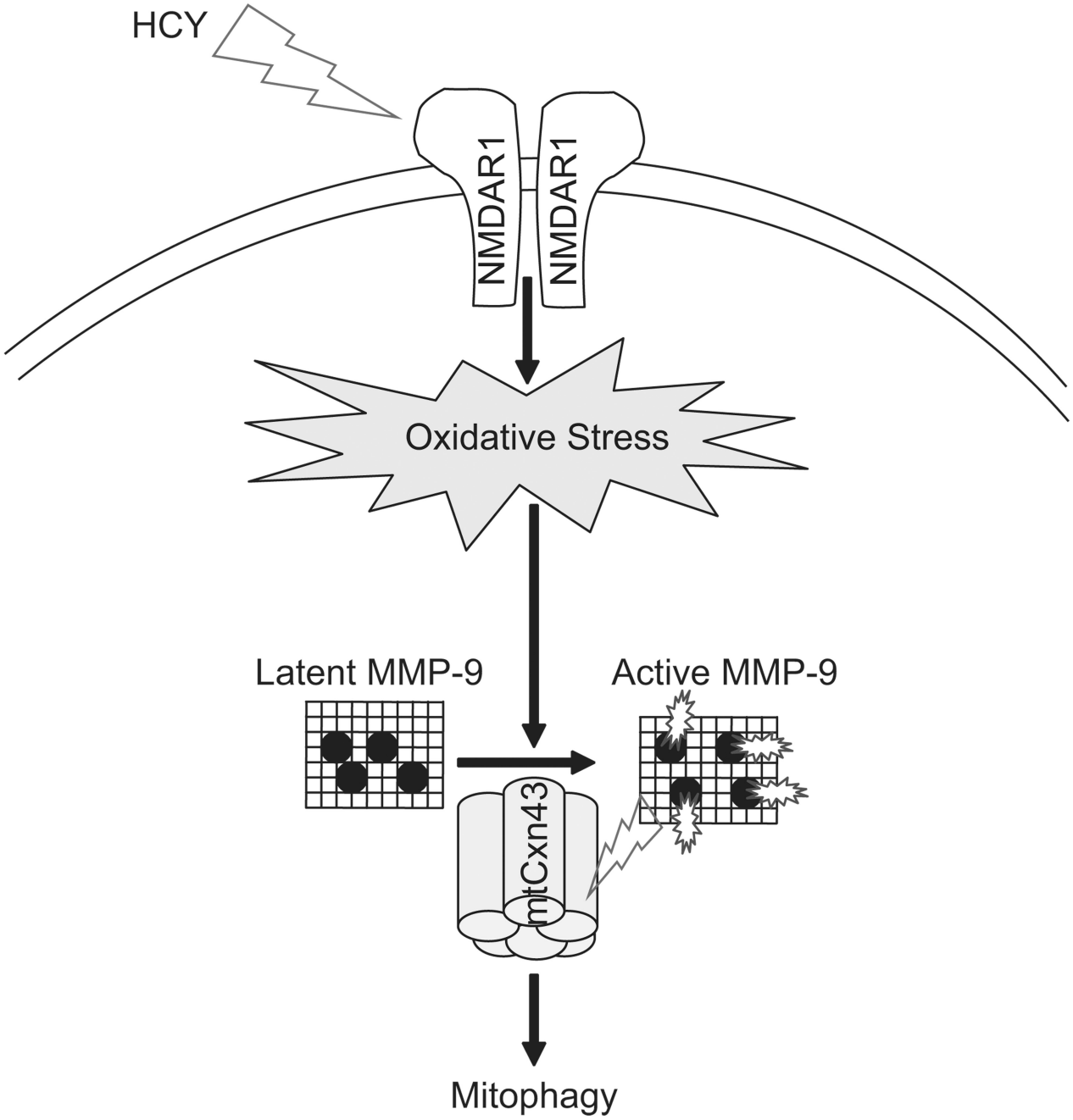

Figure 8.
Schematic presentation of the activation of NMDA-R1 by Hcy and induction of mitochondrial oxidative stress and activation of latent MMP-9 during pathogenesis of autophagy/mitophagy. The mitochondrial translocation and degradation of MMP-9 mediated connexin-43 lead to an increase in mitochondrial permeability transition pore, mitophagy and a decrease in mitochondrial oxygen consumption.